Scientia Iranica F (2018) 25(3), 1835–1848

Sharif University of Technology
Scientia Iranica
Transactions F: Nanotechnology
http://scientiairanica.sharif.edu

Investigation into thermally activated migration of fullerene-based nanocars

A. Nemati, A. Meghdari*, H. Nejat Pishkenari, and S. Sohrabpour

Nano Robotics Laboratory, Center of Excellence in Design, Robotics, and Automation (CEDRA), School of Mechanical Engineering, Sharif University of Technology, Tehran, Iran.

Received 23 April 2017; received in revised form 27 December 2017; accepted 23 April 2018

KEYWORDS
Fullerene;
Nanocar;
Molecular machines;
Nanotruck;
Molecular dynamics;
Diffusive motion.

Abstract. The rotational and translational motions of nanocars and nanotrucks as well as their motion regimes at different temperatures are investigated. In recent years, few similar types of molecular machines have been simulated. In contrast to previous studies, which have used the Rigid-Body Molecular Dynamics (RBMD) method, an all-atom model and classic atomistic dynamics have been employed in this paper to achieve better accuracy. Our results demonstrated that the flexibility of the chassis and its attachment to the gold surface played an important role in the motion of a nanocar. In fact, a heavier and more flexible nanocar chassis reduces its speed compared to a nanotruck. In addition, the results of simulations were compared with the available data in experimental studies carried out in recent years, and an acceptable agreement between the simulation results and experiments was observed. It was found that both molecules had three different regimes of motion, and the translational and rotational motions did not correlate. Results of this paper increase the knowledge and understanding of thermally driven fullerene-based nanocars and can be used to help with the design of nanomachines with high controllability and maneuverability.

1. Introduction

With the rapid progress in nanotechnology, manipulation of nanoscale materials has become very attractive. Many researchers attempt to fabricate small manipulators capable of high speed. There have been numerous theoretical studies and much experimental research is being done in this field. Nowadays, many methods are available for the manipulation of one molecule or a cluster of atoms on a surface. But, all of them have drastic drawbacks. Most of available methods work on merely one or a few particles, simultaneously [1]. Also, most of them are by some orders of magnitude bigger than the manipulated payloads [1].

Inspired by some natural molecular motors, like Kinesin, a lot of investigations have been conducted to fabricate manipulators whose sizes are in the same order of the manipulated payload [2,3]. For instance, James Tour et al. [1,4-11] succeeded in synthesizing molecular motors or machines which were capable to manipulate other atoms or molecules. Because of the similarities between these molecular motors and real cars, two types of them are named nanocars and nanotrucks [1,4,7-9]. In the first generation of the mentioned nano-machines, C_{60} was used as a wheel. Most nano-machines, such as the nanocar, nanotruck, and Z-car, have four wheels; however, a three-wheel nanomachine, called trimer, was also fabricated [4]. In the next generation, p-carborane-based wheels were developed in several nanocars with different shapes of chassis and even more wheels. Nanocaterpillars, nanocoopers, and angled nanocars are samples of carborane-wheel nanocars [7]. The tiny size of these

*. *Corresponding author. Tel.: +98 21 66165541*
E-mail address: meghdari@sharif.edu (A. Meghdari).

doi: 10.24200/sci.2018.20321

molecular machines gave them a considerable advantage. We can use numerous nanocars simultaneously to carry several billions of atoms or molecules or manipulate a relatively large payload [1,7,12].

Since several nanocars can be synthesized and put into operation simultaneously, they have attracted much attention as molecular machines with unique features. However, before putting these machines into operation, comprehensive understanding of their motion is necessary. Profound knowledge of their motional behavior in different conditions is essential before employing them to manipulate different payloads. Nanocar motion can be observed by STM (Scanning Tunnel Microscopy). Measurement of nanocar motion is significantly time-consuming and expensive; hence, few experimental studies have been carried out to investigate it. Two of the most important experimental studies on the motion of the nanocar family were performed by Shirai et al. [10] and Zhang et al. [11]. In their research, they investigated the motion of some fullerene-wheel and a few carborane-wheel nanocars on a gold substrate. They examined the motion of nanocars at different temperatures. Also, in some cases, they investigated the effect of electric field on nanocar motion.

It should be noted that only a few images can be captured in a minute and many details of the motion will not be revealed using STM. Considering the drawbacks of experimental measurements, it seems that computational simulation techniques are more appropriate for exploring motion of these molecular motors in different conditions. So far, the motion of only a few kinds of fullerene-wheel nano-machines, such as the nanotruck, trimer, and Z-car, has been simulated by Akimov et al. [5] and Konyukhov et al. [13,14]. In their research, they considered the nanocar as four rigid C_{60} wheels connected to a rigid chassis. Both of the mentioned investigations, based on the explained simplifying assumptions, increased the speed of simulations. However, it should be noted that assumption of rigidity decreases the model accuracy and many details of nanocar motion remain unknown. Some carborane-wheel and adamantine-wheel nanocars were simulated by the Kolomeisky group [6]. In another study, Akimov and Kolomeisky examined nanocar motion in the presence of an electric field. They took into account the charge transfer between the nanocar and gold substrate in their simulations [15].

The rigid body molecular dynamics technique conceals the effect of chassis flexibility on nanocar motion. In addition, the attachment of the chassis to the substrate is not adequately demonstrated using this method. A short report on a study of nanotruck and nanocar motions, performed by our group, was previously released [16]. In that paper, only the diffusion coefficient of translational motion was investigated and different aspects of motion, such as rotation and effect of wheels and chassis on the mobility of nanocar and nanotruck, were not addressed.

As mentioned above, the effect of chassis dimension on nanocar mobility has not been appropriately studied. Also, different regimes of nanocar motion were not comprehensively noted in previous research. Since both the nanocar and nanotruck have fullerene-based wheels, comparison of C_{60} and nanocar motions will give us a profound understanding of the motion of these machines and may bring out a correlation between C_{60} and nanocar or nanotruck motions. C_{60} is a well-known molecule and many experimental and computational studies about its motion have been performed in the recent years. For example, Nasiri Sarvi et al. [17] investigated the static and vibrational behavior of C_{60}. Also, there are many studies on the interaction and visualization of the C_{60}, graphene, and nanotubes in different conditions [18-20].

In this study, we investigate the motions of a nanotruck and a nanocar synthesized by Sasaki et al. [7] and Shirai et al. [4]. To analyze the effect of temperature on the motion, different simulations were conducted at different temperatures using classic atomistic dynamics method. By using this technique, we could achieve more accurate data and revealed more details about the motion regime of the mentioned molecules. We also investigated how the nanocar motion was affected by the attachment of chassis to the substrate. Rotation of nanocars was studied individually and finally, a correlation between the motions of the wheels, nanotruck, and nanocar was obtained. It should be mentioned that, recently, the motion of the nanocar and the nanotruck on the nonplanar surface has been studied by Nemati et al. [21].

Schematic views of a nanocar and nanotruck are presented in Figure 1. The nanotruck with its relatively stiff chassis was about 2 nm × 3 nm, while the overall dimension of the nanocar was about 3 nm × 4 nm and its chassis was completely flexible [1,4]. The nanotruck had four nitrogen atoms in its chassis. Due to the high electronegativity of nitrogen, the nanotruck had the potential to attach to and transport other molecules [7]. Scanning tunneling microscopy was used in the experimental measurement of the nanocar motion on the gold substrate. Gold substrate is a good choice for the STM imaging because of its high stability and conductivity. Motion of these molecular machines was simulated on a gold substrate in order to compare the experimental data and simulation results.

2. Simulation setup

We simulated motion of the nanotruck and the nanocar at different temperatures employing atomistic dynamics. Simulations were performed in a temperature range

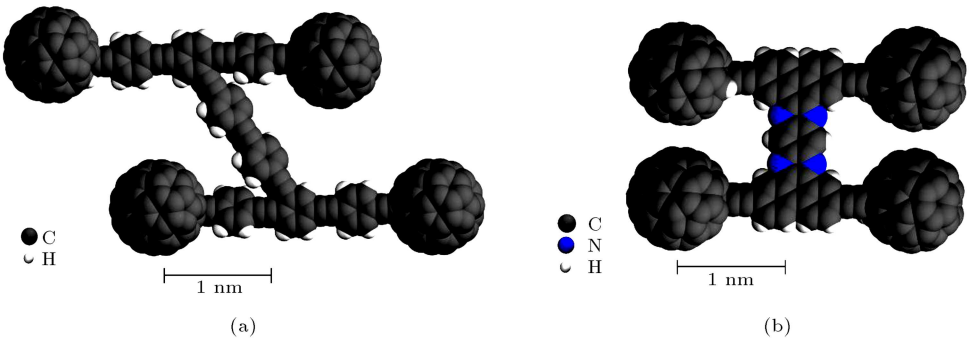

Figure 1. Top view of a fullerene-based molecular machine with four wheels: (a) Nanocar, the size of the flexible-chassis machine is approximately 3 nm × 4 nm, (b) nanotruck, the chassis is practically rigid and due to the presence of nitrogen atoms in the chassis, it can potentially be attached to and carry other molecules. Its size is about 2 nm × 3 nm. In both molecules, the carbon, hydrogen, and nitrogen atoms are shown in gray, white, and blue, respectively.

of 50 K to 600 K to demonstrate the effect of temperature on the mobility of both molecules. Substrate size was set to $18a \times 18a \times 3a$, where a is the gold lattice constant and considered to be 4.078 Å [22]. The normal direction to the gold surface was set to (100) with respect to the FCC crystalline direction. The nanocar or nanotruck was placed on top of the gold substrate and the bottom layer of atoms in the substrate was set rigid. Periodic boundary conditions in the horizontal directions were used to practically obtain an infinite substrate. An EAM alloy potential was used to model the interaction between gold atoms [23-25]. It is a very accurate potential for modeling of FCC metals [26]. A Molecular Mechanics (MM) force field was employed to model interaction among atoms inside the nanotruck and the nanocar [27]. Bonds and angle terms are considered in the harmonic style as follows:

$$E_{\text{bond}} = K_b(r - r_0)^2, \tag{1}$$

$$E_{\text{angle}} = K_a(\theta - \theta_0)^2. \tag{2}$$

In Eq. (1), K_b is the bond stiffness, and r and r_0 are the bond distance and equilibrium bond distance, respectively. In Eq. (2), K_a is the angle stiffness, and θ and θ_0 are the angle and equilibrium angle, respectively. Dihedral term style is presented in Eq. (3) [28]:

$$E_{\text{dihedral}} = \frac{1}{2}K_{d1}(1+\cos\varphi) + \frac{1}{2}K_{d2}(1-\cos 2\varphi) + \frac{1}{2}K_{d3}(1+\cos 3\varphi) + \frac{1}{2}K_{d4}(1-\cos 4\varphi), \tag{3}$$

where φ represents the dihedral angle, and K_{d1} to K_{d4} are the torsion stiffness parameters. Improper terms are neglected in the simulations. Parameters used in this potential are calculated based on an MM3 force field and presented in Table 1 [29-33].

Simulations were performed using a Large-scale Atomic/Molecular Massively Parallel Simulator (LAMMPS) solver [34] and visualization of results was done by VMD software. Temperature of the substrate and the nanocar was controlled using two individual

Table 1. Parameters used in simulation of the nanocar and nanotruck.

Bonds parameters		
K_b(ev/Å^2)	r_0 (Å)	**Description**
48.6652	1.212	C2 C2
30.8837	1.313	C2 CA
25.1593	1.392	CA CA
14.35	1.101	CA H
34.596	1.260	CA NA
Angles parameters		
$K_a(ev/\text{rad}^2)$	θ_0	**Description**
1.46619	π	C2 C2 CA
1.34141	$2\pi/3$	C2 CA CA
1.34141	$2\pi/3$	CA CA CA
1.12304	$2\pi/3$	CA CA H
1.34141	$2\pi/3$	CA CA NA
1.34141	0.638 π	CA NA CA

Dihedrals parameters				
$K_{d1}(ev)$	$K_{d2}(ev)$	$K_{d3}(ev)$	$K_{d4}(ev)$	**Description**
0	4.34E-05	0	0	CA C2 C2 CA
0	4.34E-05	0	0	C2 C2 CA CA
0	0.650451	0	0	C2 CA CA CA
0	0.650451	0	0	C2 CA CA H
–0.0403	0.208144	0	0	CA CA CA CA
0	0.234379	0.046	0	CA CA CA H
0.0433	0.650451	0	0	CA CA CA NA
0	0.390271	0	0	H CA CA H
0	0.650451	0	0	H CA CA NA
0	0.433634	0	0	NA CA CA NA
0	0.433634	0	0	CA CA NA CA

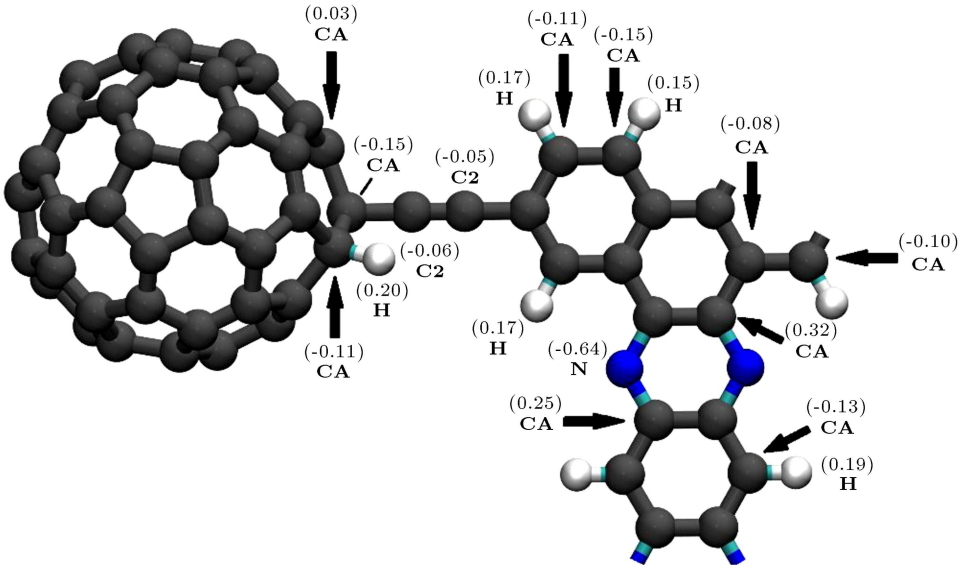

Figure 2. Different types of carbon atoms and charge distribution considered in the nanotruck.

Nose-Hoover thermostats. For adequate exploration of the phase space, 6 individual simulations were conducted for 8 nanoseconds and the time step was assumed to be 1 fs. Also, the system was relaxed to 200,000 steps. To achieve better accuracy, two different types of carbon were considered in the chassis of the nanocar and nanotruck. A section from the nanotruck chassis is shown in Figure 2. As shown in Figure 2, according to the location of a carbon atom in the chassis and its hybridization, it is considered to be of type "CA" or "C2." Carbon atoms with sp hybridization were considered as C2 and carbon atoms with sp^2 or sp^3 hybridization were considered as CA.

To calculate charge distribution in the nanocar and nanotruck molecules, the first principle theorem, i.e. Restricted Hartree-Fock (RHF), was used. Calculations were performed employing the NWChem 6.5 package and 6-31G**(d,p) basis set [35]. Charge distribution in the nanotruck is depicted in Figure 2. Due to the absence of any electric field, charge transfer between the nanomachines and gold substrate was neglected. Since the gold substrate is electrically neutral, considering electric charge for atoms in the nanotruck or nanocar does not significantly affect the motion of these nanomachines on the gold substrate. Charge distribution in the nanocar and nanotruck is symmetric and other carbon atoms, as indicated in Figure 2, have nearly zero charge.

Van der Waals interactions of H-Au, C-Au, and N-Au are modeled employing the Lennard-Jones 6-12 potential. Interaction parameters between gold and both types of carbon atoms are considered to be the same. LJ potential can be expressed as follows:

$$E_{\mathrm{LJ}} = 4\varepsilon\left[\left(\frac{\sigma}{r}\right)^{12} - \left(\frac{\sigma}{r}\right)^{6}\right], \tag{4}$$

Table 2. Parameters of LJ potential.

Description	ε (mev)	σ (Å)
C-Au	0.01273	2.994
H-Au	0.01315	2.611
N-Au	0.01423	2.886
C-C	0.00190	3.460
N-N	0.00230	3.244
H-H	0.00204	2.673
C-N	0.00213	3.350
C-H	0.00197	3.647
N-H	0.00220	2.958

where ε is the well depth of the potential, r is the equilibrium distance of gold and carbon atoms, and σ is the potential at equilibrium position. The cut-off radius of 13 Å was set for all LJ interactions. Parameters of LJ potential are listed in Table 2 [36].

3. Translational and rotational motion

Figure 3 depicts the nanocar motion trajectory during the simulation time from 50 K to 600 K. As plotted in Figure 3(a), there are not substantial displacements at temperatures lower than 200 K. The nanocar starts to skitter with short-range movements when the temperature increases to 300 K; however, it does not experience a substantial movement on the surface. In Figure 3(b), we can see that the displacement of the nanocar does not exceed 20 Å during 8 ns at 300 K, which is even less than the size of the nanocar. Thus, we can say that the nanocar is relatively motionless at 300 K.

The nanocar movement range grows when the temperature increases to 400 K, but the nanocar does not yet have significant displacement, so its motion

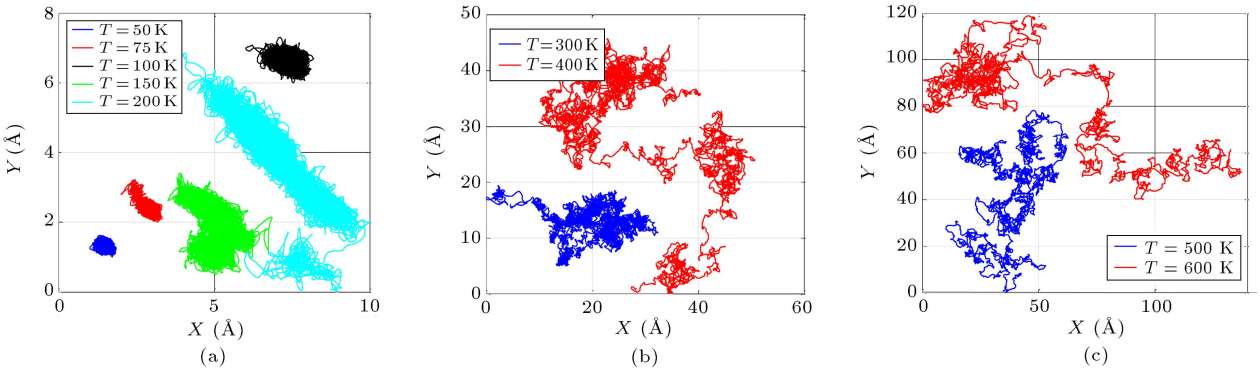

Figure 3. Nanocar trajectory for 8 ns: (a) The nanocar is almost stationary below temperatures of 200 K, (b) it has short-range fluctuations between 200 K and 400 K, and (c) nanocar has long-range movement at temperatures higher than 500 K.

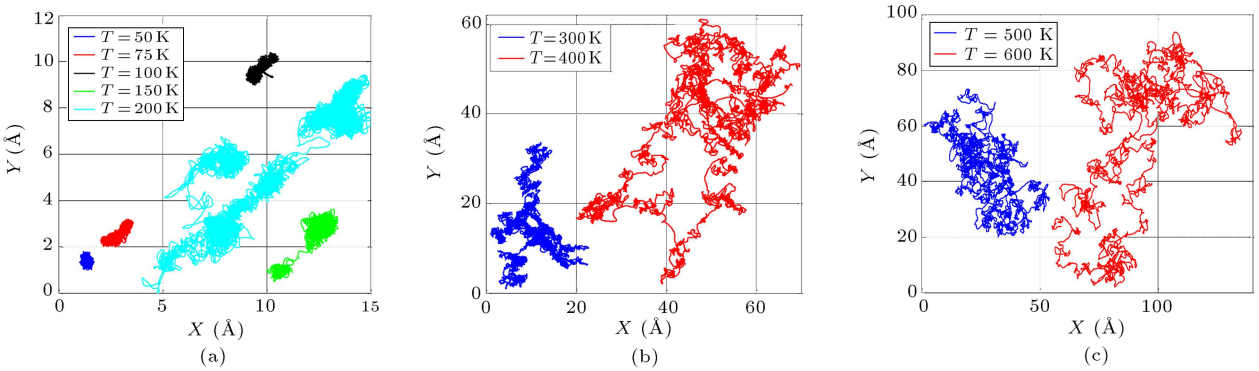

Figure 4. Nanotruck trajectory during an 8 ns simulation: (a) It is almost immobile below 200 K, (b) it shows fluctuation motion between 200 K and 400 K, and (c) nanotruck motion regime converts to long-range movements above 500 K.

type may still be considered as short-range fluctuations.

As shown in Figure 3(c), the nanocar has considerable motion at 500 K and can travel far distances in the simulation time. Therefore, we can assume that the nanocar has long-range movement at 500 K. If we simulate the system evolution for a few microseconds, the nanocar also travels substantially at 400 K; however, the translational motion of the nanocar is still insignificant compared to the nanocar motion at 500 K. We should mention that there is no distinct border between the long-range motion and short-range fluctuation. As shown in Figure 3(c), the nanocar moves easily on the surface at 600 K. It travels very long distances on the surface in the simulation time at this temperature.

In the following, the nanotruck motion at different temperatures is studied. Figure 4 depicts the nanotruck trajectory from 50 K to 600 K during the simulation.

As shown in Figure 4, the nanotruck is nearly stationary at temperatures lower than 200 K. In this temperature range, the nanotruck became stuck in its position. When the temperature increases to 300 K, the nanotruck is no longer stationary and has short-range fluctuation motion. Fluctuation range of the nanotruck increases as the temperature rises to 400 K, but its motion is not yet significant. The movement of the nanotruck at 400 K in the simulation time is in the same order of its size. At 500 K, the nanotruck freely moves on the surface and can travel long distances during the simulation time; and finally, its movement becomes very fast and ballistic at 600 K.

Based on the results illustrated in Figures 3 and 4, the nanotruck and nanocar motion types are very similar. Despite the existence of some inequalities between nanocars and nanotrucks, their similarities are undeniable. Both have four fullerene wheels and their dimensions and masses are in the same order; hence, similar motion regimes are not unexpected.

Mean Square Displacement (MSD) is a very useful parameter for understanding nanocar motion. One of the best parameters to describe diffusive motion of a particle is the diffusion coefficient, which is derived from the MSD. MSD is expressed as follows [37]:

$$\mathrm{MSD}(t) = < |r(t) - r(0)|^2 >, \tag{5}$$

where r is the position vector of the nanocar center of mass and $<>$ represents averaging over all simula-

tions performed at a certain temperature. Diffusion constant, D, is defined as the slope of the MSD plot:

$$D = \lim_{t\to\infty} \frac{1}{bt} < |r(t) - r(0)|^2 >, \quad (6)$$

where b is 6 for three-dimensional and 4 for two-dimensional motions. In this paper, we are interested in studying the horizontal (two-dimensional) motion of a nanocar on the surface; thus, we ignore the vibrations of the nanocar in the vertical direction.

To have an accurate estimation of MSD, numerous simulations should be conducted and an average of all of them should be obtained. An alternative method is to conduct a relatively long time simulation and divide the trajectory into many individual shorter-time trajectories. We performed 6 different and relatively long simulations, and divided each one into sixty smaller trajectories. The mean square displacement of the nanocar was calculated using these new shorter-time trajectories. Using MSD and Eq. (6), the diffusion coefficient was computed. Diffusion coefficients of the nanocar at different temperatures are plotted in Figure 5.

As mentioned before, by considering the simulation results depicted in Figures 3 and 4, we can introduce three distinct regimes for nanocar motion on gold substrate:

1. Being stuck with no movement;
2. Short-range fluctuations;
3. Long-range movements.

According to Figure 5, changing the regime of motion from 1 to 2 is adequately clear. We observe that the nanocar and nanotruck motion regimes change from 1 to 2 at 200 K. But there is no clear border between long-range translational movements and short-range fluctuations. In general, we saw that the motion

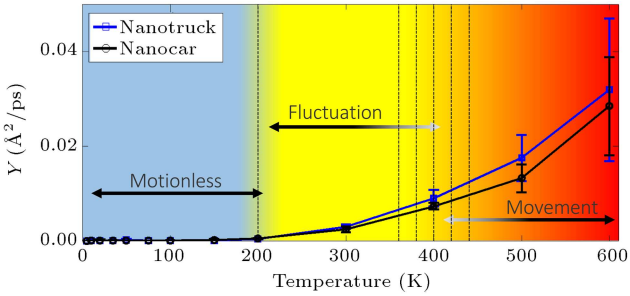

Figure 5. Diffusion coefficient for translational motions of the nanocar and nanotruck at different temperatures on gold substrate. Based on the diffusion constant, it can be concluded that the nanocar and nanotruck are immobile at 200 K and lower temperatures. Also, there is no distinct border between fluctuation regimes and long-range movements for either the nanocar or the nanotruck.

regime of the nanocar switched from short-range fluctuations to long-range translational movements somewhere around 400 K. The most important result from Figure 5 is that the nanotruck moves more easily than the nanocar at almost every temperature.

In recent years, only a few experimental studies have been performed on nanocar motion. One of the important investigations was done by Zhang et al. [11]. They experimentally studied nanocar free motion in ultra-high vacuum on gold substrate. Our purpose is to evaluate the validity of our simulation results based on a comparison with the experimental observations. If there is good agreement between the simulation results and experimental observations, we can conclude that it is possible to obtain more detailed information by extended analysis of simulation results.

Zhang et al. [11] concluded that the nanocar remained motionless at temperatures lower than 200°C and started moving on the gold substrate when the temperature was 200°C. At 200°C, nanocar motion was a combination of rotation and translation. At high temperatures, like 300°C, STM imaging was not possible due to the very quick motion of the nanocar.

By considering the results of our simulations, we can see that the nanocar has no noticeable motion at 400 K and lower temperatures. At 500 K (227°C), it has significant motion and a long-range translational motion regime. Also, at 600 K (327°C), it travels very long distances over the simulation time. Comparing simulation results and experimental observations, we can conclude that there is acceptable agreement between the simulation results and experimental observations.

Akimov et al. [5] and Konyukhov et al. [13,14] studied the motion of several types of fullerene-wheel nanocars using the Rigid Body Molecular Dynamics (RBMD) method to simulate the motion of the molecules. They assumed that the nanocar had a rigid chassis, which was attached to four rigid wheels. As a result, this method might have some limitation and some aspects of motion might not be revealed. The motion of nanotrucks and Z-cars was specifically investigated by Konyukhov et al. They reported that the diffusion coefficient of a nanotruck on a gold surface at 300 K was about 0.2 Å^2/ps [14]. They also reported that the diffusion coefficient for Z-car motion was about 0.11 Å^2/ps in the same conditions.

Considering the results plotted in Figure 5, it is shown the all-atom model predicts the diffusion coefficient for a nanotruck to be about 0.003 Å^2/ps at 300 K. This clearly implies that the RBMD method predicts the motion of nanotruck much quicker than all-atom molecular dynamics does.

Results from experimental studies [10,11] show that the nanotruck is immobile at room temperature. The all-atom model states that a nanotruck has small-

range motion at this temperature. But, considering the results from the rigid body molecular method, the nanotruck should have fast and long-range motion at 300 K. Therefore, there is not good agreement between the RBMD results and experimental observations, and the all-atom model agrees better with the experiments.

Akimov et al. also investigated the motion of a trimer and nanotruck using the rigid body molecular dynamics method [5]. The results were same as the above. They compared the rigid body molecular dynamics and all-atom model very briefly. They also reported that the RBMD method predicted the diffusion coefficient of a nanotruck, or other types of fullerene-wheel nanocars, 1-2 orders of magnitude higher than the all-atom model.

To better understand nanotruck and nanocar motions, we studied the wheels and chassis effects on the motion, individually. Since C_{60} plays a significant role in the motion of nanocars, it is reasonable to study fullerene movement on a gold substrate before any analysis of the nanocar motion. Motion of C_{60} has been investigated by many researchers in different conditions and on many substrates [38-40]. Also, exploration of C_{60} motion on a gold substrate has previously been performed by Nejat Pishkenari et al. [41,42] in 2015. Herein, we have compared the nanocar and the C_{60} motions at some different temperatures. The motion trajectory of the nanocar and C_{60} is displayed in Figure 6 at different temperatures.

According to Figure 6, it can be deduced that maneuverability of C_{60} on the gold substrate is significantly higher than that of the nanocar. In a similar way, it can be demonstrated that the nanotruck is considerably less agile than C_{60}. The nanocars and the nanotrucks interact with the gold substrate mostly via the fullerene wheels. In what follows, we aim to relate maneuverability of these nanomachines to the C_{60}.

Assume four hypothetical similar random variables x_1, x_2, x_3, and x_4 with a normal distribution, zero average value, standard deviation of S, and $< ||X_1|| >= ... =< ||X_4|| >= \mu$ in which $< ||x_1|| >$ indicates the average of the absolute values of x_1 parameter. By averaging the four mentioned variables, we will have $= \frac{1}{4}\sum(x_1 + x_2 + x_3 + x_4)$, $< X >= 0$, $< ||X|| >= \mu/2$, and a standard deviation of $X = S/2$ [43].

C_{60} motion on a gold substrate is diffusive. C_{60} speed distribution on a gold substrate is almost normal and C_{60} average velocity is almost zero. According to the previous discussion, if we attach four C_{60}s together, the resulting assembly will also have zero mean velocity, but its mean speed is half the C_{60}'s mean speed.

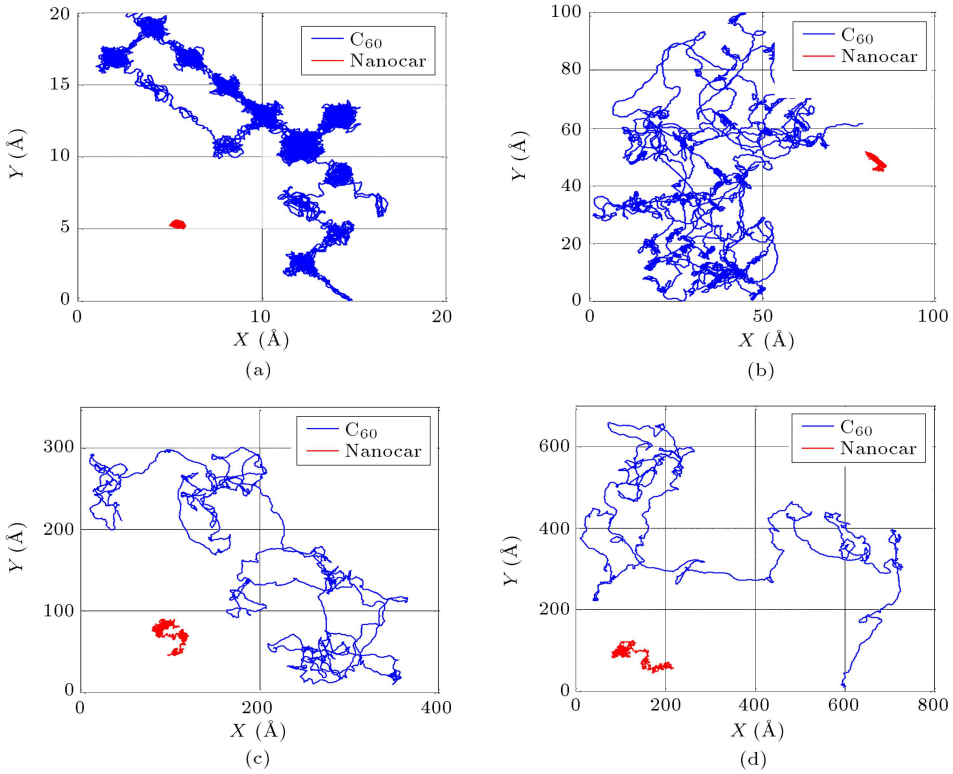

Figure 6. Trajectory of a nanocar and C_{60} during a simulation time of 8 ns at different temperatures: (a) 50 k, (b) 200 k, (c) 400 k, and (d) 600 k. Maneuverability of the nanocar on the gold substrate is significantly less than that of the C_{60}. This is mainly because of the nanocar mass, inertia, and its four wheels. The flexibility of a nanocar has only a minor effect in lowering the mobility of the nanocar.

Now, consider an imaginary nanocar which has four fullerene wheels. It has a rigid and massless chassis with zero interaction with the gold substrate. A complex of $4\times C_{60}$ was studied by Konyukhov et al. in 2010 [13]. They investigated the correlation between fullerene wheels, specifically in rotational motion. They reported that there was a weak correlation among the motions of wheels in the $4\times C_{60}$ complex. Nejat Pishkenari et al. [41] also noted that the rotational motion of C_{60} was independent from its translational motion. Considering both of these studies, it can be concluded that the wheels of a nanocar or nanotruck have individual and independent motion.

Based on the previous discussions, in this hypothetical nanocar, random motions of the four fullerene wheels neutralize each other's speed, which causes the imaginary nanocar speed to become half the wheels speed. Also, the standard deviation of the speed of this imaginary nanocar will be 1/2 the wheels speed standard deviation. Normally, when decreasing the speed, the nanotruck or the nanocar motion range on the surface will dramatically decrease. Therefore, we conclude that the fluctuations of wheels compensate for the effects of each other. This means that the motion range and the speed of C_{60} are much more than those of the nanocar or the nanotruck.

The mean speeds of the nanotruck and nanocar reported in the above studies and the mentioned imaginary nanocar are plotted in Figure 7 at different temperatures. As mentioned before, the imaginary nanocar average speed is calculated based on the results obtained from simulation of C_{60} motion in the same conditions. As plotted in Figure 7, the average speeds of the nanocar and nanotruck are less than that of the imaginary nanocar at almost every temperature. Mean speed was calculated by averaging over 6 different simulations. The standard deviation of the mean speed for the nanocar and nanotruck is also plotted in the figure inset. The small value of the standard deviation demonstrates that the mean speeds of the nanocar and nanotruck have almost the same value in different simulations.

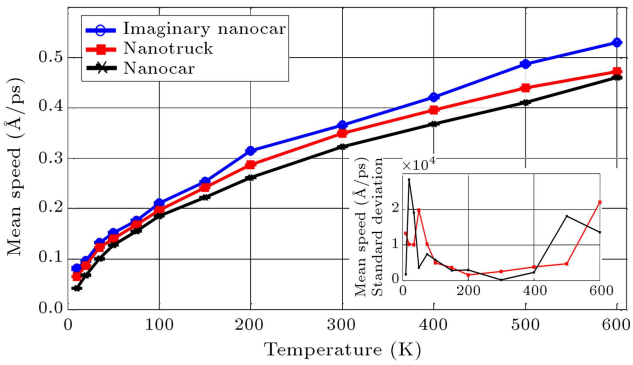

Figure 7. Mean speeds of a nanotruck, a nanocar, and an imaginary fullerene-wheel molecular machine. The imaginary nanocar with a rigid, massless, non-interactive chassis is faster than the nanotruck or nanocar. Inset shows the standard deviation of mean speed for different simulations for both nanocar and nanotruck.

As shown in Figure 8, the attraction between the chassis of the nanotruck and the gold surface causes it to stick to the substrate. This prevents effective motion of the nanotruck and nanocar and reduces their mobility. Therefore, the mobility of the imaginary nanocar is more than those of the reported nanocar and nanotruck because of their rigid, inactive, and massless chassis.

As shown in Figure 7, the speed of the nanocar is less than that of the nanotruck; but as mentioned in the previous section, the mobility of the nanotruck is more than that of the nanocar. Hence, the difference in their motion ranges should come from differences in their chassis, because both of these molecular machines have fullerene wheels. Figure 9(a) depicts different

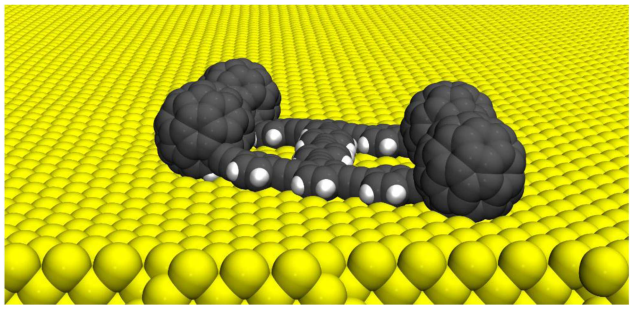

Figure 8. Attraction of chassis to gold causes it to attach to the substrate. Attachment of chassis reduces the motion agility of the nanocar and nanotruck. It also causes a distortion of the nanocar axle.

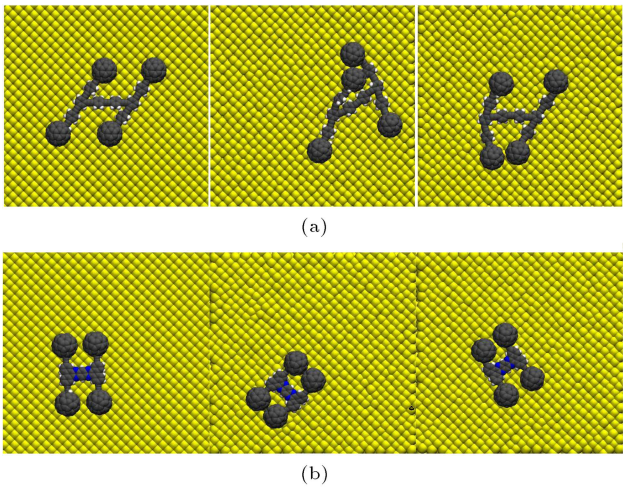

Figure 9. (a) Chassis of the nanocar and (b) chassis of the nanotruck during simulation at 400 K. The chassis of the nanotruck is relatively rigid, but the nanocar chassis is quite flexible. The flexibility of the chassis may dampen nanocar energy, slowing down its motion.

snapshots of the chassis of the nanocar during its motion at 400 K. This figure shows that its chassis was completely flexible. Whereas, as plotted in Figure 9(b), the chassis of the nanotruck remained almost rigid during simulation. Flexibility of the nanocar chassis will dampen nanocar energy. Thus, it is expected that the speed of the nanotruck will be more than that of the nanocar. Furthermore, because of the heavier chassis of the nanocar, its motion requires more energy. Thus, we can conclude that the flexibility of chassis and its interaction with the surface make a molecular motor sluggish. Using these results, we predict that similar machines with more wheels and heavier chassis will have less mobility than lighter ones with fewer wheels.

As shown in Figure 7, the motion regime of these machines is mainly governed by the wheel behavior. We are looking for a way to predict the motion of nanocars and nanotrucks using C_{60} or vice versa. We suggest that the diffusion coefficient of these molecules is a suitable parameter to define a relationship between the motions of C_{60} and a nanocar or nanotruck. As shown in Figure 10(a), the diffusion coefficient of the nanocar at 500 K is equal to the diffusion coefficient of C_{60} at 130 K. Therefore, we predict that the motion range of a nanocar at 500 K is similar to motion range of C_{60} at 1300 K. Also, the diffusion coefficient of nanotruck motion at 500 K is equivalent to the diffusion coefficient of C_{60} motion at 145 K. Trajectory of the C_{60} and nanocar, respectively, at 150 K and 500 K for a simulation time of 8 ns is plotted in Figure 10(b). Figure 10(c) also shows the motion trajectory of C_{60} and a nanotruck at 150 K and 500 K, respectively.

As depicted in Figure 10(b) and (c), the motion regime of a nanocar and nanotruck at 500 K is very similar to the motion of C_{60} at 150 K. According to Figure 7, we can conclude that the diffusion coefficient diagram is a suitable tool to figure out the motion of the nanocar or nanotruck by analyzing motion of C_{60} and vice versa.

In the previous sections, the translational motions of nanocar and nanotruck were studied. In the next step, we will investigate the rotational motion of these molecular machines. Our goal is to study the rotation of a nanocar around the vertical axis (yaw angle), which is depicted in Figure 11. Yaw angle of the nanocar during simulation time at 150 K and higher temperatures is plotted in Figure 12.

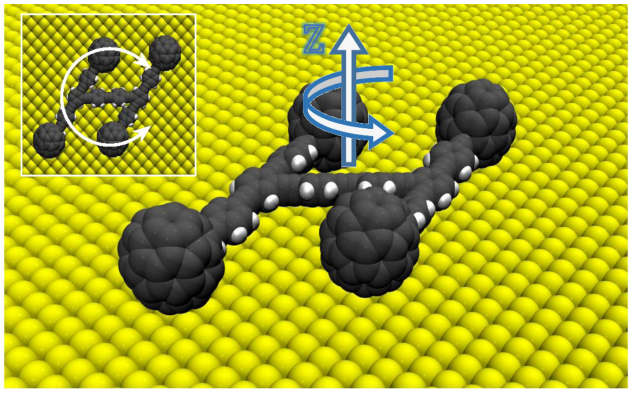

Figure 11. A demonstration of the nanocar rotation around a vertical axis (Z axis) or yaw angle. The inset presents a top view of the nanocar rotation about the vertical axis.

According to Figure 12(a), at 150 K and 200 K, the nanocar has no noticeable rotation around the vertical axis. Raising the temperature to 300 K increases the nanocar ability to rotate around the vertical axis. At this temperature, the nanocar rotates nearly 2 rad in the simulation time. When the temperature is 400 K and higher, the nanocar is clearly able to rotate. For a better understanding of rotational motion of the nanocar, we use MSD and a diffusion computing constant for the yaw angle of the nanocar, similar to the previously described method for translational motion. We divided the whole simulation into 60 independent shorter periods and applied averaging to all of them. The diffusion constant for the yaw angle of the nanocar at different temperatures is plotted in Figure 13. To compare the rotational motions of the

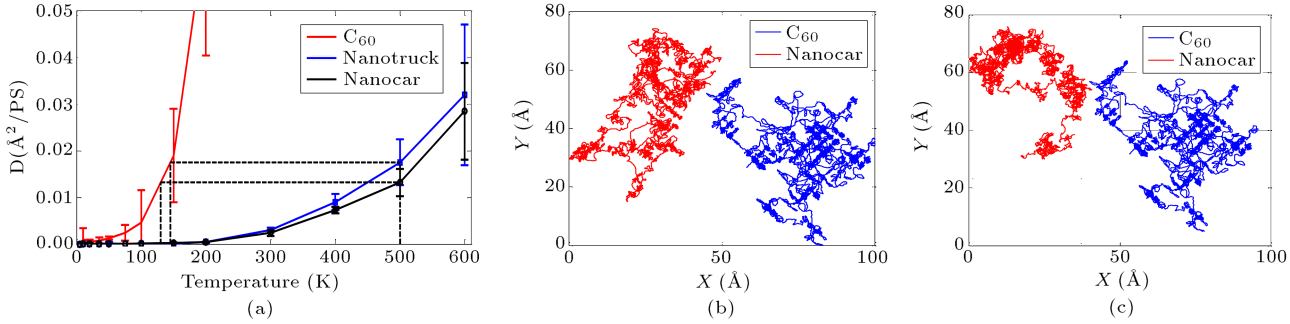

Figure 10. (a) Diffusion coefficients of C_{60}, nanocar, and nanotruck at different temperatures. Using this diagram, we can predict that the motion of the nanocar and nanotruck at 500 K is similar to that of C_{60} at 130 K and 145 K, respectively. (b) Trajectory of C_{60} at 150 K and the nanotruck at 500 K in a simulation time of 8 ns. Similarity of motion ranges leads us to believe that the diffusion coefficient diagram is a powerful tool to predict the motion of a nanocar from that of C_{60} or vice versa. (c) Trajectory of C_{60} at 150 K and the nanocar at 500 K in a simulation time of 8 ns.

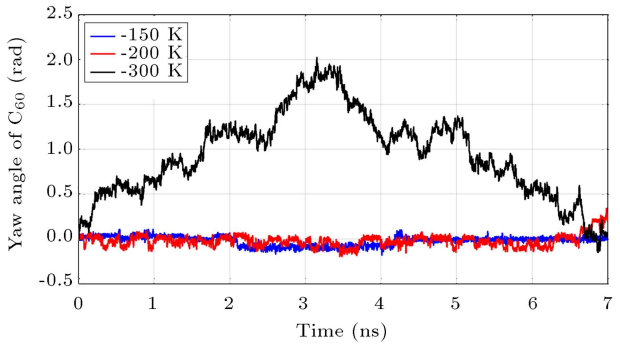

(a)

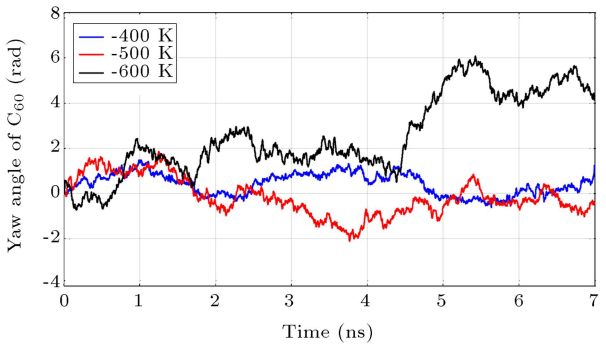

(b)

Figure 12. Yaw angle of nanocar: (a) at 300 K and lower temperatures, and (b) at 400 K and higher temperatures. At 150 K and 200 K, the nanocar has short-range oscillation around the vertical axis. At 300 K, the nanocar can rotate around the vertical axis. At 400 K and higher temperatures, the ability of the nanocar to rotate increases.

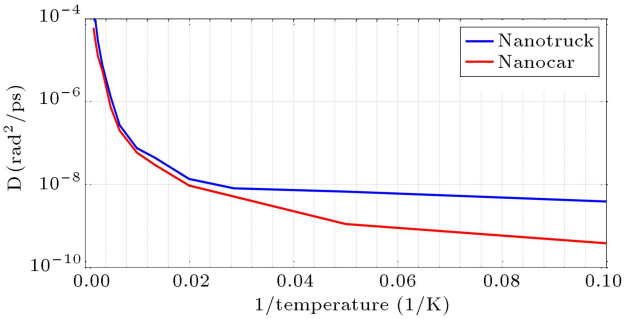

Figure 13. Arrhenius analysis of the diffusion coefficients of rotational motions of the nanocar and nanotruck. Similar to translational motion, the ability of the nanocar is less than the nanotruck in rotational motion.

nanocar and nanotruck, the diffusion constant for the nanotruck is also depicted in Figure 13. Based on the Arrhenius analysis depicted in Figure 13, there is a clear change in the regimes of the nanocar and nanotruck rotational motions. We can deduce that the nanocar and nanotruck have two different regimes: Low-amplitude rotational oscillations at 200 K and lower temperatures, and rotation around the vertical axis at 300 K and higher.

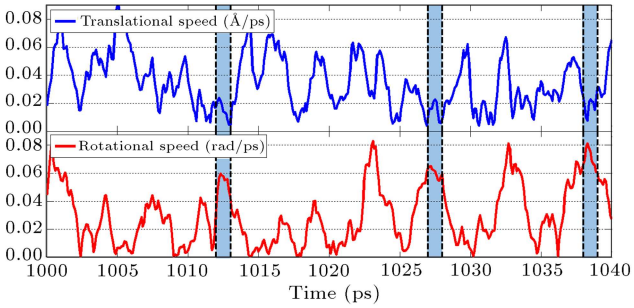

Figure 14. Translational and rotational speeds of the nanotruck during the simulation for a short window of time at 500 K. At the marked period of time, the nanotruck has near zero speed in translation, but it has significant rotational speed. There is no correlation between translational and rotational speeds.

4. Holonomic and directional motion

In the next step, we studied the rotational and translational motions of a nanotruck during its motion on the substrate. Figure 14 shows the rotational and translational speeds of the nanotruck for a short period of time. As shown in this figure, there is a period of time that the nanotruck translational speed is near zero, but it has significant rotational speed; therefore, we can conclude that the nanotruck rotational and translational speeds are independent. Independency in rotation and translation means that despite the similarities that nanocars and nanotrucks have with real-world cars, they do not have a nonholonomic constraint on their motion in contrast to a four-wheel car.

We can also see that the nanocar can freely rotate on the substrate independently from the translational motion. Creators of these nanomachines expected them to have directional motion; we will investigate the directional motions of nanocar and nanotruck in the next section.

As seen in Figure 11, the nanocar chassis is quite flexible during its motion. Major deformation of the chassis makes it hard to distinguish the direction of the nanocar and so it is not feasible to attribute a displacement to transverse motion or the motion along the chassis. But, it is possible to study directional motion of the nanotruck due to its relatively rigid chassis.

As shown in Figure 15, the velocity of the nanotruck chassis in a transverse direction is considered as V_t and will be called "transverse speed". Also, the velocity along the chassis is denoted by V_t and will be called "longitudinal speed". As depicted in the inset of Figure 15, the rigid section of the chassis is considered when calculating the chassis direction and speed.

In Figure 16, the transverse and longitudinal speeds of a nanotruck chassis are depicted for a short period of time. At the highlighted sections,

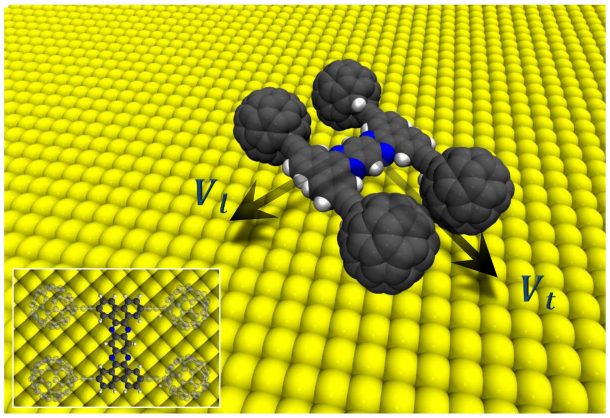

Figure 15. Longitudinal speed V_t is the speed of the nanotruck chassis along the chassis direction. Transverse speed V_l is the speed of the chassis in the transverse direction. The picture inset shows the rigid section of the chassis considered when calculating the chassis speed and direction.

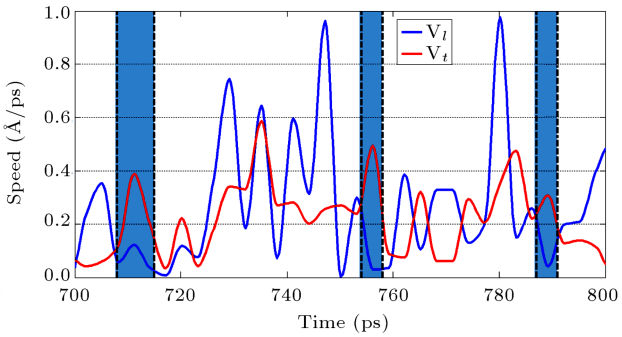

Figure 16. Longitudinal and transverse speeds of the nanotruck chassis in the simulation for a short-time window at 500 K. At these specified periods of time, transverse speed is significantly larger than longitudinal speed. This confirms the nonexistence of constraint on the nanotruck motion on the gold substrate. It seems that longitudinal speed is more than transverse speed for most periods of time, which shows the tendency of the nanotruck to move along its chassis rather than in a transverse direction.

the transverse speed of the chassis is much more than its longitudinal speed. This confirms the fact that there is no constraint on the nanotruck motion. Figure 16 also illustrates that the transverse speed of the nanotruck chassis is less than its longitudinal motion, for most periods of time. The means of transverse and longitudinal speeds of the nanotruck chassis during the simulation time are calculated at different temperatures and depicted in Figure 17.

As shown in Figure 17, the longitudinal speed of the nanotruck chassis (V_l) is significantly more than its transverse speed (V_t). Although the nanotruck does not show a clear directional motion, it has a tendency to move along its chassis rather than to sideways. Figure 17 shows the ratio of V_l/V_t at different

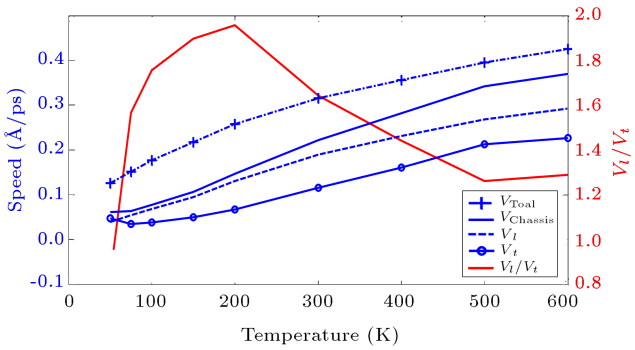

Figure 17. Mean value of the longitudinal speed is more than that of the transverse speed at all temperatures. Descending behavior of V_t/V_l for temperatures higher than 200 K shows that increasing the temperature will diminish the directional motion and increase the diffusive motion. The total speed of the nanotruck is more than the chassis speed, hence the chassis slows down the motion of the nanotruck.

temperatures. Decrease in this ratio is indicative of more diffusive motion and increase in this parameter is a good sign of directional motion. At 200 K, where the nanotruck starts to move on the surface, V_l/V_t reaches its maximum value. At higher temperatures, this ratio begins to decrease. This means that when the temperature rises, directional motion of the nanotruck will diminish and the nanotruck has more ability to move in the transverse direction.

In Figure 17, the speed of nanotruck, including its wheels, is also plotted. Comparing the speeds of the nanotruck chassis and the whole nanotruck reveals that the chassis speed is less than the whole nanotruck speed at every temperature. Attachment to the substrate makes it hard for the chassis to move. Moreover, C_{60} wheels are very agile and quick, so they have a high speed compared to either the chassis or the whole nanotruck. Thus, when we attach highly active C_{60} wheels to the slow chassis, the final assembly speed will be intermediate. As we concluded before, the chassis slows down the motion of the nanotruck and this is confirmed by the results depicted in Figure 7.

5. Conclusion

In this paper we investigated the motions of a nanotruck and a nanocar on a gold substrate at different temperatures using MD with all-atom details. Nanocars and nanotrucks had three distinct motion regimes on a gold substrate. They were both almost motionless at temperatures lower than 200 K. They had a low amplitude fluctuation without considerable displacements at more than 200 K and less than 400 K. They moved freely on the substrate at temperatures higher than 500 K. Their motion regimes were long-range movements at high temperatures. A switch

between the motion regimes was obvious at 200 K, but no distinct border was observed between short-range fluctuation and long-range movements. The available experimental results show that substantial motion of a nanocar starts at 200°C, but at 300°C, the nanocar moves too fast to be imaged. These observations are in good agreement with our simulation results.

Comparing the results of the all-atom molecular dynamics and Rigid Body Molecular Dynamics (RBMD) methods shows that rigid body molecular dynamics predicts the diffusion coefficient of nanocar or nanotruck 1-2 orders of magnitude higher than all-atom molecular dynamics does. Also, based on the comparison with experimental observations, the results of all-atom molecular dynamics are in good agreement with experiments.

Because of its stiffer, smaller, and lighter chassis, the motion range of the nanotruck is more than that of the nanocar. We compared the motions of nanocar and nanotruck with the motion of C_{60} as well as imaginary nanocar including 4 C_{60} wheels and a massless, relatively rigid, inactive chassis. The results showed that the flexibility of the chassis and its attachment to the substrate would decrease both the nanocar and nanotruck motion abilities. With regard to this information, we can predict that similar molecular machines with more wheels or heavier chassis are less agile than a nanotruck.

Regarding rotational motion, the nanotruck and the nanocar had low-amplitude oscillations around the vertical axis at 200 K and lower temperatures, while they were able to rotate freely at temperatures higher than 300 K. At 300 K, the nanocar could not move significantly on the substrate, but could easily rotate. This showed that translational and rotational motions of the nanocar and nanotruck were independent and rotational motion was more likely to happen than translational motion. Studying rotational and translational motions led us to the conclusion that unlike real-world cars, there was no nonholonomic constraint on the motions of the nanocar and nanotruck. Translational and rotational motions of these molecular machines did not correlate with each other and could occur independently. At 500 K and higher temperatures, nanotruck and nanocar motions were a combination of translational and rotational movements.

Directional motion of the nanotruck was studied at different temperatures, and it was found that a nanotruck could independently and simultaneously move both along and perpendicular to its chassis. But, the nanotruck tendency to move along its chassis was greater than its tendency to move in a direction perpendicular to its chassis. At higher temperatures, the nanotruck could move more freely in the direction perpendicular to its chassis and its motion was less directional. Due to the substantial deformation of the nanocar chassis, it was hard to distinguish a specific direction for the nanocar; thus, it was not quite possible to investigate directional motion of a nanocar.

The results of this paper provide appropriate understanding of the motion of two of the most basic fullerene-based nanocars. They can be used to predict general aspects of the motion of other nanocars with similar architecture. Also, the results of this research can be used in the design of new fullerene-based nanocars with improved controllability and maneuverability.

References

1. Vives, G. and Tour, J.M. "Synthesis of single-molecule nanocars", *Accounts of Chemical Research*, **42**(3), pp. 473-487 (2009).
2. Kinbara, K. and Aida, T. "Toward intelligent molecular machines: directed motions of biological and artificial molecules and assemblies", *Chemical Eeviews*, **105**(4), pp. 1377-1400 (2005).
3. Popov, V.L. "Nanomachines: Methods to induce a directed motion at nanoscale", *Physical Review E*, **68**(2), p. 026608 (2003).
4. Shirai, Y., Osgood, A.J., Zhao, Y., Yao, Y., Saudan, L., Yang, H., Yu-Hung, C., Alemany, L.B. , Sasaki, T., Morin, J.F., Guerrero, J.M., Kelly, K.F., and Tour, J.M. "Surface-rolling molecules", *Journal of the American Chemical Society*, **128**(14), pp. 4854-4864 (2006).
5. Akimov, A.V., Nemukhin, A.V., Moskovsky, A.A., Kolomeisky, A.B., and Tour, J.M. "Molecular dynamics of surface-moving thermally driven nanocars", *Journal of Chemical Theory and Computation*, **4**(4), pp. 652-656 (2008).
6. Chu, P.-L.E., Wang, L.-Y., Khatua, S., Kolomeisky, A.B., Link, S., and Tour, J.M. "Synthesis and single-molecule imaging of highly mobile adamantane-wheeled nanocars", *ACS Nano*, **7**(1), pp. 35-41 (2012).
7. Sasaki, T., Morin, J.F., Lu, M., and Tour, J.M. "Synthesis of a single-molecule nanotruc", *Tetrahedron Letters*, **48**(33), pp. 5817-5820 (2007).
8. Sasaki, T., Osgood, A.J., Alemany, L.B., Kelly, K.F., and Tour, J.M "Synthesis of a nanocar with an angled chassis. Toward circling movement", *Organic Letters*, **10**(2), pp. 229-232 (2008).
9. Sasaki, T. and Tour, J.M. "Synthesis of a dipolar nanocar", *Tetrahedron Letters*, **48**(33), pp. 5821-5824 (2007).
10. Shirai, Y., Osgood, A.J., Zhao, Y., Kelly, K.F., and Tour, J.M. "Directional control in thermally driven single-molecule nanocars", *Nano Letters*, **5**(11), pp. 2330-2334 (2005).
11. Zhang, J., Osgood, A., Shirai, Y., Morin, J.F., Sasaki, T., Tour, J.M., and Kelly, K.F. "Investigating the motion of molecular machines on surfaces by STM: The

nanocar and beyond", in *Nanotechnology IEEE-NANO 7th IEEE Conference* on (2007).

12. Shirai, Y., Minami, K., Nakanishi, W., Yonamine, Y., Joachim, C., and Ariga, K. "Driving nanocars and nanomachines at interfaces: From concept of nanoarchitectonics to actual use in worldwide race and hand operation" *Japanese Journal of Applied Physics*, **55**(11), p. 1102A2 (2016).
13. Konyukhov, S.S., I.V. Kupchenko, A.A. Moskovsky, A.V. Nemukhin, A.V. Akimov, and A.B. Kolomeisky, "Rigid-body molecular dynamics of fullerene-based nanocars on metallic surfaces", *Journal of Chemical Theory and Computation*, **6**(9), pp. 2581-2590 (2010).
14. Konyukhov, S., Artemov, N., Kaliman, I., Kupchenko, I., Nemukhin, A., and Moskovskii, A. "Diffusion of fullerene-based nanocars on the surface of a gold crystal", *Moscow University Chemistry Bulletin*, **65**(4), pp. 219-220 (2010).
15. Akimov, A.V. and Kolomeisky, A.B. "Unidirectional rolling motion of nanocars induced by electric field", *The Journal of Physical Chemistry C*, **116**(42), pp. 22595-22601 (2012).
16. Nemati, A., Pishkenari, H.N., Meghdari, A., and Shorabpour, S. "Nanocar & nanotruck motion on gold surface", *International Conference on Manipulation, Automation and Robotics at Small Scales (MARSS)*, (2016).
17. Nasiri Sarvi, M. and Ahmadian, M.T. "Static and vibrational analysis of fullerene using a newly designed spherical super element", *Scientia Iranica*, **19**(5), pp. 1316-1323 (2012).
18. Adeli, M., Madani, F., and Sasanpour, P. "Synthesis of graphene/gold hybrid nanomaterials by poly(ethylene glycol) linkers", *Scientia Iranica*, **21**(3), pp. 1163-1173 (2014).
19. Nejat Pishkenari, H. and Meghdari, A. "Tip geometry effects in surface characterization with amplitude modulation AFM", *Scientia Iranica*, **17**(F1), pp. 27-34 (2010).
20. Crisan, O. "Molecular nanostructures onto functionalized semiconductor surfaces: An in-situ atomic force microscopy study", *Scientia Iranica*, **17**(F2), pp. 154-161 (2010).
21. Nemati, A., Pishkenari, H.N., Meghdari, A., and Shorabpour, S. "Directing the diffusive motion of fullerene-based nanocars using nonplanar gold surfaces", *Physical Chemistry Chemical Physics*, **20**(1), pp. 332-344 (2018).
22. Dutta, B. and Dayal, B. "Lattice constants and thermal expansion of gold up to 878°C by X-ray method", *Physica Status Solidi (b)*, **3**(3), pp. 473-477 (1963).
23. Foiles, S., Baskes, M., and Daw, M. "Embedded-atom-method functions for the fcc metals Cu, Ag, Au, Ni, Pd, Pt, and their alloys", *Physical Review B*, **33**(12), p. 7983 (1986).
24. Finnis, M. and Sinclair, J. "A simple empirical N-body potential for transition metals", *Philosophical Magazine A*, **50**(1), pp. 45-55 (1984).
25. Daw, M.S. and Baskes, M.I. "Embedded-atom method: Derivation and application to impurities, surfaces, and other defects in metals", *Physical Review B*, **29**(12), p. 6443 (1984).
26. Stukowski, A., Sadigh, B., Erhart, B., and Caro, A. "Efficient implementation of the concentration-dependent embedded atom method for molecular-dynamics and Monte-Carlo simulations", *Modelling and Simulation in Materials Science and Engineering*, **17**(7), 075005 (2009).
27. Burkert, U. and Allinger, N.L., *Molecular Mechanics*, **177**, American Chemical Society Washington, DC. (1982).
28. Watkins, E.K. and Jorgensen, W.L. "Perfluoroalkanes: Conformational analysis and liquid-state properties from ab initio and Monte Carlo calculations", *The Journal of Physical Chemistry A*, **105**(16), pp. 4118-4125 (2001).
29. Allinger, N.L. "Conformational analysis. 130. MM2. A hydrocarbon force field utilizing V1 and V2 torsional terms", *Journal of the American Chemical Society*, **99**(25), pp. 8127-8134 (1977).
30. Allinger, N.L., Chen, K., and Lii, J.H. "An improved force field (MM4) for saturated hydrocarbons", *Journal of computational chemistry*, **17**(5-6), pp. 642-668 (1996).
31. Allinger, N.L., Yuh, Y.H., and Lii, J.H. "Molecular mechanics. The MM3 force field for hydrocarbons. 1", *Journal of the American Chemical Society*, **111**(23), pp. 8551-8566 (1989).
32. Lii, J.H. and Allinger, N.L. "Molecular mechanics. The MM3 force field for hydrocarbons. 3. The van der Waals' potentials and crystal data for aliphatic and aromatic hydrocarbons", *Journal of the American Chemical Society*, **111**(23), pp. 8576-8582 (1989).
33. Lii, J.H. and Allinger, N.L. "Molecular mechanics. The MM3 force field for hydrocarbons. 2. Vibrational frequencies and thermodynamics", *Journal of the American Chemical Society*, **111**(23), pp. 8566-8575 (1989).
34. Plimpton, S. "Fast parallel algorithms for short-range molecular dynamics", *Journal of Computational Physics*, **117**(1), pp. 1-19 (1995).
35. Valiev, M., Bylaska, E.J., Govind, N., Kowalski, K., Straatsma, T.P., Van Dam, H.J., Wang, D., Nieplocha, J., Apra, E., and Windus, T.L. "NWChem: a comprehensive and scalable open-source solution for large scale molecular simulations", *Computer Physics Communications*, **181**(9), pp. 1477-1489 (2010).
36. Heinz, H., Vaia, R., Farmer, B., and Naik, R. "Accurate simulation of surfaces and interfaces of face-centered cubic metals using 12-6 and 9-6 Lennard-Jones potentials", *The Journal of Physical Chemistry C*, **112**(44), pp. 17281-17290 (2008).
37. Qian, H., Sheetz, M.P., and Elson, E.L. "Single particle tracking. Analysis of diffusion and flow in two-dimensional systems", *Biophysical Journal*, **60**(4), p. 910 (1991).

38. Abramo, M.C., Caccamo, C., Costa, D., Pellicane, G., and Ruberto, R. "Atomistic versus two-body central potential models of C_{60}: A comparative molecular dynamics study", *Physical Review E*, **69**(3), p. 031112 (2004)

39. Lohrasebi, A., Neek-Amal, M., and Ejtehadi, M. "Directed motion of C 60 on a graphene sheet subjected to a temperature gradient", *Physical Review E*, **83**(4), p. 042601 (2011).

40. Neek-Amal, M., Abedpour, N., Rasuli, S., Naji, A., and Ejtehadi, M. "Diffusive motion of C60 on a graphene sheet", *Physical Review E*, **82**(5), p. 051605 (2010)

41. Pishkenari, H.N., Nemati, A., Meghdari, A., and Sohrabpour, S. "A close look at the motion of C_{60} on gold", *Current Applied Physics*, **15**(11), pp. 1402-1411 (2015).

42. Hosseini Lavasani, S.M., Nejat Pishkenari, H., and Meghdari, A. "Mechanism of 1,12-dicarba-closo-dodecaborane mobility on gold substrate as a nanocar wheel", *The Journal of Physical Chemistry C*, **120**(26), pp. 14048-14058 (2016).

43. Johnson, R.A. and Wichern, D.W., *Applied Multivariate Statistical Analysis*, **4**, Prentice Hall Englewood Cliffs, NJ (1992).

Biographies

Alireza Nemati received his MS degree in Mechanical Engineering from Sharif University of Technology. He is currently PhD student in Nano Robotic Laboratory of the Center of Excellence in Design, Robotics, and Automation (CEDRA) at Sharif University of Technology.

Ali Meghdari received his PhD degree in Mechanical Engineering from the University of New Mexico in 1987. Then, he joined the robotics group of Los Alamos National Laboratory as a Post-Doctoral research collaborator. In 1988 (1366), he joined Sharif University of Technology (SUT) in Tehran. Professor Meghdari has performed extensive research in various areas of robotics; social and cognitive robotics, mechatronics, bio-robotics, and modelling of biomechanical systems. He has supervised over 75 MSc theses, 18 PhD dissertations, and 5 Post-Docs, and has published over 250 technical papers in refereed international journals and conferences. He has been the recipient of various scholarships and awards, the latest being the 2012 Allameh Tabatabaei distinguished professorship award by the National Elites Foundation of Iran (BMN); the 2001 Mechanical Engineering Distinguished Professorship Award from the Ministry of Science, Research and Technology (MSRT) in Iran; and the 1997 ISESCO Award in Technology from Morocco. During 1996-2000, he chaired the School of Mechanical Engineering and during 2001-2010, he was the Vice-President of Academic Affairs at Sharif University of Technology. He is currently the Director of the Centre of Excellence in Design, Robotics and Automation (CEDRA). He is on the editorial board of various engineering journals, an affiliate member of the Iranian Academy of Sciences (IAS), and a Fellow of the American Society of Mechanical Engineers (ASME).

Hossein Nejat Pishkenari earned his BSc, MSc, and PhD degrees in Mechanical Engineering from Sharif University of Technology in 2003, 2005, and 2010, respectively. Then, he joined the department of Mechanical Engineering at Sharif University of Technology in 2012. Currently, he is directing the nano-robotics Laboratory and the corresponding ongoing research projects in the multidisciplinary field of nanotechnology.

Saeed Sohrabpour is an Iranian academic and was the 15th chancellor of Sharif University of Technology from 1997 to 2010. He graduated from University of Tehran and later, received his PhD in Mechanical Engineering from UC Berkeley.